Summer 2019

Evaluating the Efficacy of Sand Fences on Dunes Impacted by Hurricanes

Michelle Harris

EVALUATING THE EFFICACY OF SAND FENCES ON DUNES IMPACTED BY HURRICANES

by

Michelle Harris

Bachelor of Science
Sam Houston State University, 2016

Submitted in Partial Fulfillment of the Requirements

For the Degree of Master of Science in

Geography

College of Arts and Sciences

University of South Carolina

2019

Accepted by:

Jean Ellis, Director of Thesis

C. Patrick Barrineau, Reader

Gregory Carbone, Reader

Cheryl L. Addy, Vice Provost and Dean of the Graduate School

ACKNOWLEDGEMENTS

I would first like to thank my advisor, Dr. Jean Ellis, and committee members Dr. Gregory Carbone and Dr. C. Patrick Barrineau for their guidance and support with this thesis. The outflow of support, time, and patience were paramount to the success of this project.

Secondly, I would like to thank those who assisted with field data collection: Jean Ellis, J. Brianna Ferguson (“contra-flow storm crew”), and Peter Tereszkiewicz. I would additionally like to extend this gratitude to all WINDlab members who provided feedback and support throughout this study, ALE, and PPH. I would also like to thank Mayra Román-Rivera for the mentoring she has provided during my graduate studies.

Finally, I would like to extend my gratitude to Ava Fujimoto-Strait, who “got me into this mess,” with her support in prior years.

ABSTRACT

Erosion is present in over 90% of the world's coastlines and poses a threat to infrastructure and natural systems. While the coastal zone is a morphologically dynamic environment, a range of engineering practices have evolved to stabilize it. Because the natural dune system serves as the first line of defense against storm activity and rising sea levels, it is often incorporated into restorative engineering practices. One popular and economical option is the utilization of sand fences. This option is readily available to homeowners and managers, with simple installation requirements. Typically measured for their ability to induce short-term dune growth, scant research has considered storm impact on sand fence installations, their persistence, and the resulting change to dune morphology.

This study evaluates the geomorphic response from sand fences resulting from the impact of high energy events, specifically Hurricanes Florence and Michael, which impacted South Carolina in 2018. A combination of cost-effective field methods were applied to calculate dune volume at two sites along a mechanical dune. Measurements compared a site with eleven sand fences and an unmodified control site. Dune volume decreased after Hurricane Florence for both sites but accreted after Hurricane Michael for the fenced site. There was differential morphologic change post-storm between the control and fenced sites, with an overall smaller volumetric loss for the fenced site.

Results from this study support the resilience of sand fences under high wind conditions as an effective strategy to aid in dune recovery and growth, suggesting that they can be emplaced prior to the storm season rather than reserved as a post-storm recovery technique. Field observations further suggest the addition of vegetation planted with sand fence installations for optimal dune growth.

TABLE OF CONTENTS

LIST OF TABLES

LIST OF FIGURES

CHAPTER 1

INTRODUCTION

Erosion leads to millions of U.S. dollars spent in mitigation to prevent landward migration of coastlines (Conathan, Buchanan, and Polefka, 2014). Dune systems serve as a natural line of defense to protect against storm impacts. Unfortunately, in many coastal locations natural dune systems have been reduced in lieu of development and infrastructure as population density continues to increase (Portz et al., 2014). In South Carolina, efforts to reduce shoreline erosion often manifest as nourishment, scraping, vegetation planting, and the installation of sand fences. While the two former methods rely heavily on municipal and federal resources, the installation of sand fences can be completed in a cost-effective manner by city managers and/or individual homeowners.

Sand fences are placed to stabilize existing dune systems or to encourage incipient dune formation. They provide a porous barrier and are installed in a wide array of positions, including shore parallel, perpendicular, or in V-shaped formations with a landward apex (Figure 1.1). Installations seek to regulate the rate of aeolian transport to reduce erosion and/or to cause sand deposition (Li and Sherman, 2015). Sand may be transported in conditions where shear velocity (u_*) exceeds threshold shear velocity (u_{*t}). As wind-blown sand is

transported, it encounters the fence slats, which decreases the wind speed. If the threshold shear velocity (u_{*t}) is no longer exceeded and transport ceases, deposition will occur on the lee side of the fence. In multidirectional wind environments, sediment will accrete on the lee side of the fence (Zaghloul, 1997).

Sand fences are a popular and cost-effective method to promote dune growth along the South Carolina coast (OCRM, 2018). Many of the original sand fences in South Carolina were placed after the 1987 January nor'easter storm (Thieler and Young, 1991). After Hurricane Hugo made landfall in South Carolina in 1989, a second suite of sand fences were emplaced and vegetation was planted to aid in dune recovery (Katuna, 1991). Remnant posts from these installations are still visible (2019) in what are now the secondary and tertiary dunes along Isle of Palms, South Carolina, which is the focus area this study (Katuna, 1991; personal communication, 2018).

Previous research has focused on sand fences that were installed post-storm to aid in dune recovery (Miller, Thetford, and Yager, 2001; Khalil, 2008). We are not aware of any published studies in South Carolina that focus on the geomorphic influence of sand fences that were installed prior to a storm and persisted afterward. Research investigating sand fence performance is of increasing importance as homeowners, managers, and municipalities now commonly install sand fences throughout the year rather than being restricted to post-storm conditions (personal communication, 2018). This study therefore investigates the morphological impacts of hurricanes on sand dunes that are fenced compared to those that are not. Specifically, this study will examine the

large- and fine-scale morphologic impact of Hurricanes Florence and Michael on a mechanical dune system that has a fenced and a control site on the Isle of Palms, South Carolina. Periods of sand transport during the study period are also predicted based on environmental conditions measured at the site.

Figure 1.1 Sand fences installed in a V-shaped formation along a South Carolina beach. The apex of the “V” is pointing towards the dune crest.

CHAPTER 2

BACKGROUND

2.1 Scraping

Beach scraping is a management technique that may stabilize or replace the primary dune ridge in the event of erosion. Heavy machinery redistributes existing sediment from the foreshore to the backshore, seaward of the existing primary dune line (Kana and Svetlichny, 1982). In South Carolina, state regulations mandate that this structure is termed an ‘emergency berm’ but on Isle of Palms, it is placed along the primary former dune line. Unlike beach nourishment, this practice alters the existing sediment budget rather than adding to it (Bruun, 1983). A modified dune, hereafter referred to as a mechanical dune, is constructed to enhance protection against wave energy and coastal erosion (Conaway and Wells, 2005).

Scraping has been widely enacted under emergency orders in South Carolina to fortify coastal communities. This practice is commonly performed to protect landward infrastructure from inundation post-storm (Katuna, 1991). However, the lasting impact on the beach remains controversial (Wells and McNinch, 1991), with the suggestion made that the construction of the mechanical dune creates a false sense of security for homeowners (Lentz et al., 2013) or should be regarded as a temporary measure (Bruun, 1983; Ellis and

Román-Rivera, 2019). Studies have focused on the morphologic, volumetric, and ecological impact of beach scraping over various temporal durations (Kana and Svetlichny, 1982; Kerhin and Halka, 1981; Peterson et al. 2000; Conaway and Wells, 2005) and have made conclusions spanning a wide spectrum when considering overall efficacy. Historically, the shape of the mechanical dune has not mimicked a natural dune system upon placement (Smyth and Hesp, 2015), which can impact the natural rate of transport. Because sediment is brought from the nearshore, it is often less sorted and can result in increased transport, erosion, and/or deflation, which inhibits dune stabilization or growth (Kerhin and Halka, 1981; Lindquist and Manning, 2001; Conaway and Wells, 2005). Increased transport rates have been reported on mechanical dunes when compared to natural dune systems post-storm, resulting in exacerbated erosion and a coarser remnant grain size (Wells and McNinch, 1991; Conaway and Wells, 2005). Similarly, a lack of deposition along a mechanical dune in comparison to a natural dune was noted after Hurricane Hugo in 1989 (Wells and McNinch, 1991), begging to question the resilience of scraped dunes to tropical cyclones. This controversy was reinforced in a more recent South Carolina-based study that found that mechanical dunes were not an optimal protection technique when compared to a natural dune system post-Hurricanes Matthew and Irma (Ellis and Román-Rivera, 2019). The impact to sediment transport within the dune system and grain size matching is often disregarded in beach scraping, which is commonly regarded as a soft engineering alternative to shoreline armoring (Bruun, 1983). From a regulatory perspective, there is a lack

of consistency regarding beach scraping (Bruun, 1983) and anchoring methods, such as the emplacement of sand fences or dune vegetation (Katuna, 1991).

2.2 Sand Fences

Records of sand fence utilization date back to the 1400's and include placement to protect roadways, guide pedestrian traffic, and to encourage dune growth and stabilization (Van der Laan et al., 1997). Fence material varies by project objective and geographic location, but can be grouped into permanent or transitory (biodegradable) categories (López and Marcomini, 2006). Typical construction materials include plastic snow fencing, individual wooden slats secured by wire, geojute material, and partially buried or fixed branches and vegetation of local availability (Mendelssohn et al., 1991; López and Marcomini, 2006; Huang and Yim, 2014).

Previous research has broadly investigated sand fence engineering to identify key structural components to increase their efficacy. For wooden slat fences, linear fence configurations installed shore parallel have the highest rates of dune accretion (Savage, 1962). When multiple parallel fenced are installed, trapping capacity increases (Lima et al., 2017). Fences are most effective with a 40-50% porosity (Hotta and Horikawa, 1990). Models generated by Zaghloul (1997) revealed that fences experiencing prevailing winds led to less deposition than those exposed to multi-directional wind environments. Nordstrom et al. (2012) noted that sand fences actively trap sediment and lead to taller dune crests than natural environments, with limited seaward dune growth.

The reported optimal fence height varies from 0.30 m (OCRM, 2018) to 0.50 m (Lima et al., 2017); many U.S. consumers rely on standard commercially available wood-slat fence rolls measuring 1.2 meters in height. The exposed height may decrease during installation, with many homeowners cutting the fence in half to extend coverage, or by partially burying them to increase initial stability. Additionally, anchoring posts create an initial gap between the fence posts and the bed. This gap structurally weakens the fence, which often leads to fence displacement or damage, but it may increase the potential height of the dune (Zaghloul, 1997).

Once installed, the impact of a sand fence on environmental conditions has been documented in reference to biotic and abiotic factors. Vegetation distribution in response to the utilization of sand fences has been detailed (Grafals-Soto, 2012) and suggestions proposed to best preserve natural biota altered by fence placement (Grafals-Soto and Nordstrom, 2009). Deposition rates and dune sizes increase when a mixed stabilization approach incorporating vegetation and sand fences is installed (Mendelssohn et al., 1991). Locations susceptible to overwash experience faster recovery rates and vegetation reestablishment when paired with sand fence installations (Miller, Thetford, and Yager, 2001).

2.3 Estimating Mass Transport

Advancements within the mechanics of aeolian sediment transport began in the 1930’s with Bagnold (Bagnold, 1936, 1941; Pye and Tsoar, 2009). This early work provided the framework for subsequent studies that connected aeolian

transport to dune formation (Pye and Tsoar, 2009). Simplistically, for aeolian sediment transport to occur, the shear velocity (u_*) exerted from surface wind must exceed the threshold shear velocity (u_{*t}) required for particle motion (Sherman and Bauer, 1993). Once motion is initiated, particles move by reptation, saltation, creep, or suspension (Pye and Tsoar, 2009). Varying wind conditions, sediment characteristics, and site-specific influences can lead to distinctive dune morphologies that transform the coastal landscape (Herrmann and Sauermann, 2000), with scales ranging from meters (hummocks) to hundreds of meters (ridges) in elevation (Psuty, 2008).

To understand this dynamic environment, researchers have modeled these variables in an effort to identify trends and predict future changes. These results are exceptionally important to coastal managers who must consider evolving coastlines, particularly those under anthropogenic influence where transport conditions may be altered through coastal armoring, recreation, or other influences (Jackson and Nordstrom, 2011).

2.4 Storm Impact on Dune Systems

High energy storm events, especially hurricanes, cause dramatic change to the coastal landscape through hydrodynamic and wind regimes (Houser et al., 2015). The susceptibility to morphologic change is often magnified on barrier islands (Sallenger, 2000).

The hydrodynamic influence of low-pressure systems often manifests through storm surge, wave run-up, and potential overwash that can be detrimental to dune systems (Houser, Hapke, and Hamilton, 2008; Long, de

Bakker, and Plant, 2014). These events can exacerbate coastal and dune erosion. Storm surge and wave run-up often undercut existing dunes and produce scours, slumps, and/or scarps. Overwash is typically responsible for deflating or removing an existing dune crest and creating depositional fans landward of the dune crest (Lindemer et al., 2010). It has been suggested that areas with a history of erosion are often more susceptible to overwash and inundation during storms (Hal and Halsey, 1991). Accelerated wind energy can deflate dune systems and create blowouts and washover fans (Claudino-Sales, Wang, and Horwitz, 2008).

The resilience of dunes relies on vegetation colonization and species, dune field width and continuity, an adequate supply of sediment available for transport, and overall island topography (Sallenger, 2000; Claudino-Sales, Wang, and Horwitz, 2008; Houser et al., 2015). Sallenger (2000) further demonstrated that resilience is dependent on the ratio between the backshore and dune height and the recorded storm surge. This relationship led to the development of a storm impact scale that has been widely adopted (Sallenger, 2000). Because factors of resilience vary by geographic location, management techniques designed to reduce storm impact vary based on necessity, environmental conditions, and temporal opportunities in the event of an approaching storm. Although sand fences are a common management technique that can be impacted by storm systems, we are not aware of prior studies assessing the morphologic change induced by fences during and after storms.

2.5 Hurricanes Florence and Michael

Hurricane Florence made landfall on September 14th, 2018 near Wrightsville Beach, North Carolina as a Category 1 hurricane with sustained winds of 40.2 m/s (NOAA, 2018). Wrightsville Beach is approximately 290 km northeast of Isle of Palms, South Carolina (IOP), the focus area of this study. Following landfall, the storm traveled westward at an average speed of 2.7 m/s. Top wind speeds recorded in Charleston, South Carolina (24 km SSW of IOP) reached 14.7 m/s on September 15th and wave heights averaged 2.9 m (National Data Buoy Center Station 8665530). The dominant wind direction in Charleston was 230 degrees (National Data Buoy Center Station 8665530). The storm produced minimal rainfall; the National Weather Service reported 1.02 mm of rainfall in Charleston between the 14th and 17th of September 2018 (NWS, 2018). The storm surge recorded in Charleston was 0.25 m, arriving during a low tide of -1.6 m (National Data Buoy Center Station 8665530).

Hurricane Michael made landfall on October 10th, 2018, near Mexico City, Florida, approximately 770 km southwest of IOP as a Category 5 hurricane with sustained winds of 69.3 m/s (NOAA, 2018). The fast-moving storm traveled northeast at 7.6 m/s (NOAA, 2018; NWS, 2018). Top wind speeds recorded in Charleston reached 17.9 m/s on October 11th, 2018, with gusts exceeding 22.4 m/s recorded on IOP (National Data Buoy Center Station 8665530; IOP, 2018). The dominant wind direction in Charleston was 203 degrees (National Data Buoy Center Station 8665530). Between October 10th and 11th, IOP experienced 27.2 mm of rainfall (NWS, 2018). The maximum recorded storm surge in Charleston was 0.56 m on October 11th (National Data Buoy Center Station 8665530).

CHAPTER 3

METHODOLOGY

3.1 Study Location

Isle of Palms is a 15.6 km long barrier island located 24 km NNE of Charleston, SC. It is part of a large barrier island chain system, bordered on the southwest by Sullivan's Island and to the northeast by Dewees Island (Figure 3.1). This Holocene barrier island spans from approximately 1.6 km wide in the northeast to less than 0.4 km near Breach Inlet in the southwest, denoting that it is a classic drumstick barrier island according to Hayes (2010

Similar to other southern South Carolina barrier islands, the Isle of Palms has a tidal range of 1.8-2.1 m (Kana, 1988; Thieler and Young, 1991). As modeled by Fico (1980), the center of the island is the primary foci for wave energy. The southwestern extent, which includes both field sites, is characterized by minimal wave energy and a long-term accretionary trend (Fico, 1980). These energetics are also reflected by the sediment bypassing from Dewees Inlet and natural trends in longshore sediment transport for the barrier island (Stephen et al., 1975).

Over the last century, Isle of Palms has been influenced by an average of 1.6 tropical cyclones per year (NOAA, 2016). To mitigate the impacts of the storms, multiple beach nourishment events have taken place (IOP, 2018).

In 2008, 845,000 cubic yards of sand was dredged and placed from 54th Ave NE to Dewees Inlet (Figure 3.1). Nourishment was completed again in 2018 when approximately 1,685,000 cubic yards was dredged and placed from 53rd Ave to Dewees Inlet (IOP, 2018). The 2008 and 2018 nourishments occurred approximately 6 km northeast of our study sites.

After Hurricane Irma made landfall on September 11th, 2017 the storm triggered the issuance of an emergency scraping order for numerous beach-dune segments along Isle of Palms, including a 217 meter long portion beginning from the 5th Avenue beach access point toward the northeast (CSE, 2017). In accordance with State Emergency Order 17-EO-HI 3, specifications mandate dimensions of an 'emergency berm' (or mechanical dune) of 1.8 m height and 6.1 m width (CSE, 2017).

Two sites were selected for study, a fenced and control, near the 5th Avenue beach access point on Isle of Palms, South Carolina (Figure 3.1 subset). Both sites are within a scraped area (mechanical dune), have a SW to NE orientation, and are assumed to be under homogenous wind and wave conditions.

3.2 Field Sites

The fenced site has a linear distance of approximately 22 m. It contained ten oblique sand fences installed on a mechanical dune (Figure 3.2A) and a shore parallel fence installed landward (Figure 3.2B). The fences were oriented from the southwest to the northeast and numbered 1 through 10 (Figure 3.3). The fences were located approximately 2.3 m apart, and their average length was 3.1 m (Figure 3.3). The control site was located 18.5 m northeast of the

fenced site and had a linear distance of 22 m. We segmented the site and generated five transects that were 5.5 m apart (Figure 3.4A). This site was also on the mechanical dune, but unlike the fenced site, there was no landward development. The landward extent of the site was delineated by the vegetation line (Figure 3.4B).

3.3 Field Methods

Data collection was conducted four days prior (09/11/2018) to and six days following (9/21/2018) Hurricane Florence's impact on IOP, which was on 09/15/2018. The post-Florence data serve as the pre-storm data for Hurricane Michael, which impacted IOP on 10/11/2018. Post-Michael data were collected two days after the storm's impact on 10/13/2018. Field-based data collection included taking dune measurements, deploying or measuring erosion pins, collecting GPS points, gathering sediment samples, and taking photographs.

To quantify and evaluate large-scale geomorphic changes, dune volume was estimated using a measuring tape and a PVC pole. The landward extent of the dune (dune width), brink, height, and slope length were measured (Figure 3.5). For the fenced site, measurements were taken on the northeast side of each oblique fence. The measuring tape was in contact with the landward anchoring pole of the fence for the ten transects. For the control site, measurements were taken along the five transects (Figure 3.6B).

Erosion pins were installed in both sites on 9/11/2018 to measure fine-scale erosion and deposition (Figure 3.6). Rebar measuring 0.6 m in length were installed flush with the sand to avoid anthropogenic interference. For the fenced

site, rebar were installed along the parallel fence (section a), dune base (section b), and dune toe (section c) (Figure 3.6A). We also used the existing fence poles as erosions pins by measuring their exposed height during each field campaign. At the control site, erosion pins were installed on 9/11/2018 along the vegetation line (section a), dune base (section b), and dune toe (section c) along the five transects (Figure 3.6). On 9/21/2018 and 10/13/2018, erosion pin (rebar and fence posts) deposition or erosion was measured to estimate volumetric change.

Photos taken during the three collection dates were used to provide a qualitative record of the changes occurring before and after each storm; namely dune migration, growth, reduction, vegetation presence, and a holistic visual assessment.

Sediment grab samples were collected at the fenced and control dune during the three data collection dates (9/11/2018, 9/21/2018, and 10/13/2018) to calculate mean grain size (D_{50}).

3.4 Data Analysis

Dune volume was estimated beginning with the protocol shown in Figure 3.7. The following four assumptions were made relative to the fenced and control site when estimating volume: (1) One volumetric value as applied to estimate partial dune volume assuming the dune was flat and had no discernable crest (“b” and “c” in Figure 3.7A); (2) if the dune changed morphologically and had a discernable crest, a different protocol was used (“a”, “b”, and “c” in Figure 3.7A) to calculate volume; (3) the dune slope length measurement (“d” in Figure 3.7A)

was assumed to be a straight line, and (4) the dune height measurement ("c" in Figure 3.7A) was the height of the back dune.

Dune volume calculations were estimated between every pair of transects at each site. For example, on Figure 3.7A, volume was calculated between transects 1 and 2, then between transects 2 and 3, etc. The summation of all the segments represents the overall dune volume. To calculate the volume of prisms "a" and "c" (Figure 3.7A), the average values were applied from adjacent transect measurements ("d" in Figure 3.5, and transect spacing (Figure 4, Figure 3.7B). To visualize the percent of volumetric change, the dune was divided into three sections. The first section, herein referred to as the "back dune," included the summation of all "a" values (Figure 3.7A). The second section, herein referred to as the "dune base," included the summation of all "b" values (Figure 3.7A). The third section, herein referred to as the "dune slope," included the summation of all "c" values (Figure 3.7A).

Erosion pin percent change values were tabulated by section and compared to dune volumes to create a holistic assessment for geomorphic change post-storm. Positive values represent accretion and negative values indicate erosion. The percent change for each erosion pin was calculated over the duration of the field study.

Sediment grab samples were dried and split to obtain a random sample of 50-100 g for each date and site. They were sieved at $\frac{1}{4}\phi$ intervals with a Ro-Tap shaker set at 10 minutes. Sediment characteristics (specifically, D_{50}) was compared between the fenced and control sites.

Wind and wave data recorded every hour were collected from the National Data Buoy Center Station 8665530, which is 11.6 km SW of the field site and the closest anemometer to the field site with data for the entire study. The anemometer at this station is 8.56 m above the surface. A scaling factor of 1.03 based on Burt (2012) was employed to adjust the measured wind speeds to a standard height of 10.0 m.

The potential for aeolian sediment transport is estimated in conditions where shear velocity exceeds threshold shear velocity ($u_* > u_{*t}$). This potential was modeled using measured mean grain sizes (D_{50}) and wind conditions. Modeling was extended to include estimations for five sediment grain classes relevant to the composition on Isle of Palms, South Carolina: very fine sand (VF; 0.063 mm), fine sand (FS; 0.125 mm), medium sand (MS; 0.250 mm), coarse sand (CS; 0.500 mm), and very coarse sand (VCS; 1.000 mm) to estimate the influence of grain size on aeolian sediment transport rate. Threshold shear velocity is estimated using Bagnold (1937):

$$u_{*t} = A\sqrt{gd\left(\frac{\rho_s - \rho}{\rho}\right)} \qquad \text{(Equation 1)}$$

where A is 0.1 under fluid transport conditions, g is acceleration due to gravity, d is mean grain size, ρ_s is grain density, ρ is air density, and u_* (shear velocity) can be estimated by the Prandtl-von Kármán equation (Law of the Wall):

$$u_* = \frac{\kappa u_z}{\ln\left(\frac{z}{z_0}\right)} \qquad \text{(Equation 2)}$$

where κ is the von Kármán constant (approximately equal to 0.4, but can change based on the intensity of saltation; c.f., Li et al., 2010), u_z is mean flow velocity at elevation z above the bed, and z_0 is the roughness length, defined here as:

$$z_0 = \frac{1}{30} d \qquad \text{(Equation 3)}$$

Minimum wind speeds necessary for $u_* > u_{*t}$ were identified as wind forcing events. Wind forcing events are presented as hours of potential transport for time periods one and two.

Precipitation data was averaged using two Community Collaborative Rain, Hail and Snow Network (CoCoRaHs) stations to identify the percentage of time that rainfall may have inhibited aeolian transport. Two stations, SC-CR-77 and SC-CR-148, were chosen based on their geographic proximity to the field site (4.5 km NNW and 6.8 km NW, respectively) and because daily precipitation records were available for the study duration. Precipitation values were averaged between the two CoCoRaHs stations. In the event of recorded precipitation, the following 24 hours were not considered as potential hours for aeolian sediment transport, regardless of the wind velocity (and corresponding u_*) readings.

Wave data were processed to identify forcing events occurring during both time periods. Forcing events are defined here as wave heights exceeding two standard deviations (Zhang et al., 2002).

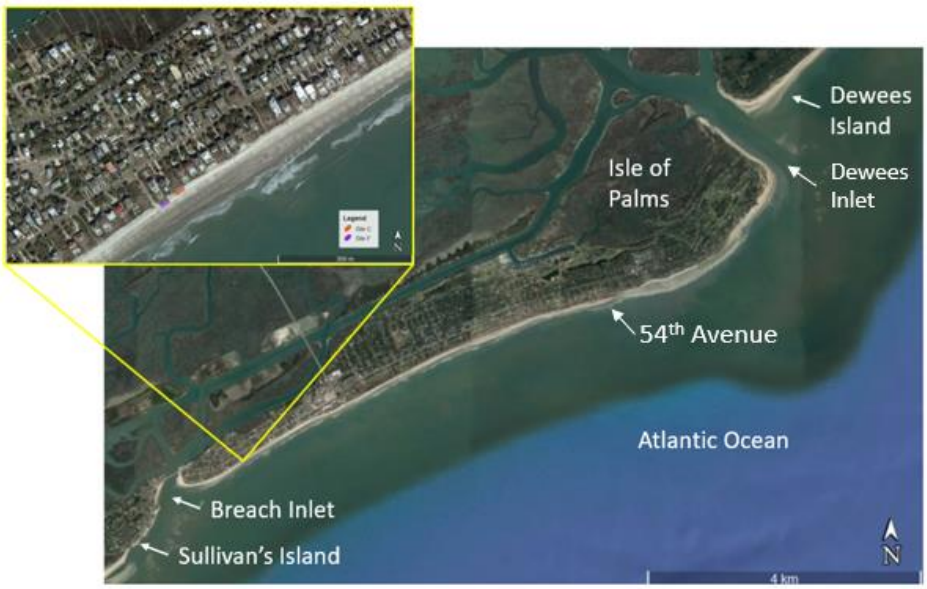

Figure 3.1. Isle of Palms, South Carolina, with subset showing both field sites NE of the beach access point at 5th Ave. Subset: Field site where the purple box is the fenced site and orange box is the control site. Source: Google Earth, 2017. Note Fences are not present in this imagery.

Figure 3.2. Photos of the fenced site taken on 9/11/18, where the wrack represented the high tide line from the recent king tide on 09/09/2018. A) View looking landward. B) View of site from southwestern extent, including the shore parallel fence (left side of image).

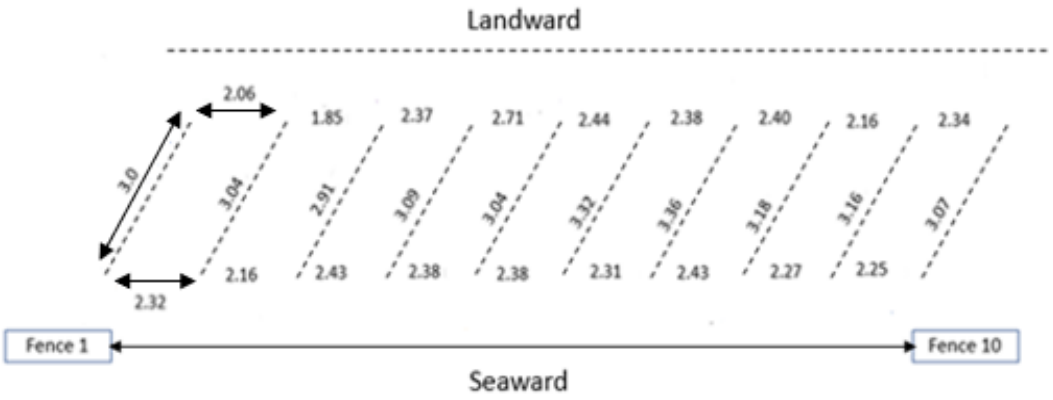

Figure 3.3. Schematic of the fenced site with measurements shown in meters. Dashed lines represent sand fences. The length of the study site was equivalent to the length of the back shore parallel fence (21.96 m). Fence numbers correspond to transect numbers (1-10).

Figure 3.4. Photos taken of the control site on 09/11/18. A) View looking landward. B) Landward extent of control site (vegetation line).

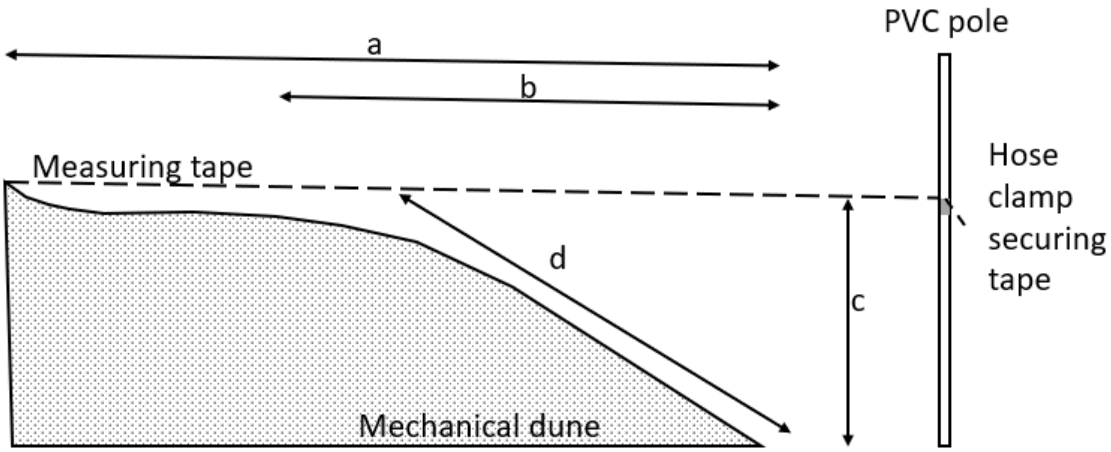

Figure 3.5. Summary of measurements using the PVC pole and measuring tape where a) is from the dune toe to the fence line/vegetation line (site dependent), b) is from the brink to the dune toe, c) is the height of the dune, and d) is the dune slope length. These measurements were gathered at both sites.

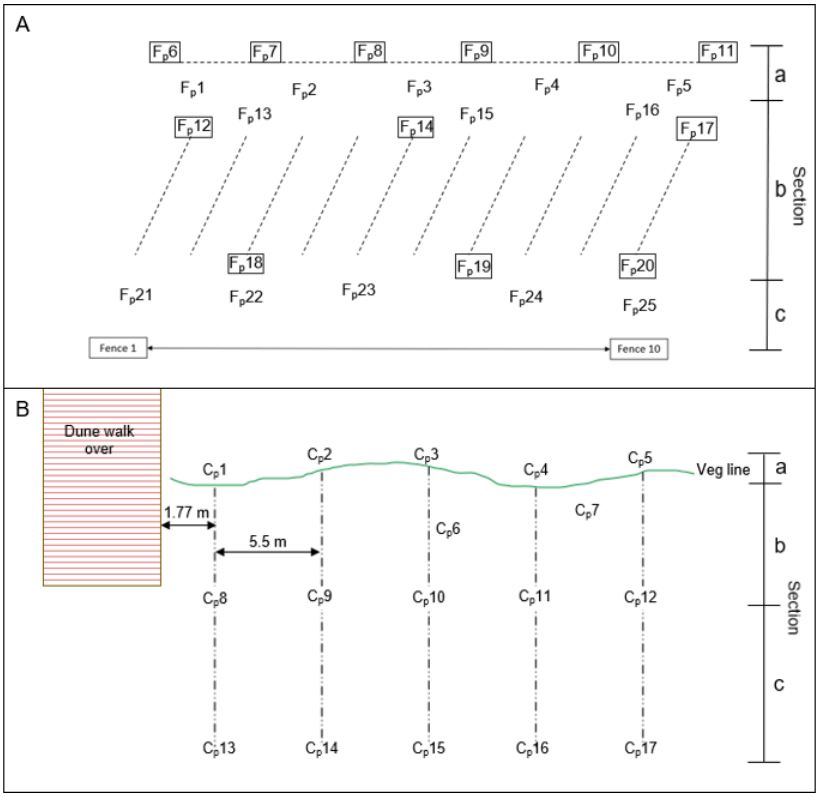

Figure 3.6. Erosion pin deployment schematics for the fenced (A) and control (B) site. Corresponding section values are designated to the right each schematic A) Fenced site where the oblique and parallel fences are shown in dashed lines and F_p (Fence pin) values are erosion pins. Boxed F_p values represent wooden fence posts. B) Control site where C_p (Control pin) rebar were installed.

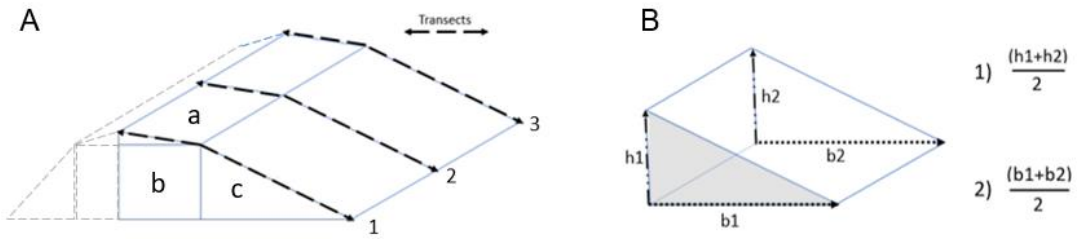

Figure 3.7. A) Volumetric schematic where total dune volume was estimated by summing the volumes of A) back dune triangular prism derived from “a”, “b”, and “c” in Figure 3.5 b) dune base rectangular prism derived from “a”, “b”, and “c” in Figure 3.5, and c) dune slope triangular prism derived from “b”, “c”, and “d” in Figure 3.5. Note: Area shown in the grey dashed lines was excluded from this study. B) Example prism used for volume calculations, where “b” represents “b” in Figure 3.5, and “h” is found using assumption 4. The average values from adjacent transects were derived to solve for the area of the prism (shown in grey) and then overall prism volume.

CHAPTER 4

RESULTS

The following results are presented for the control and fenced sites during and directly after Hurricanes Florence (9/11/18-9/21/18) and Michael (9/21/18-10/13/18), with the former referred to as time period one and the latter as time period two.

4.1 Wind and Wave Analysis

For time period one, the average wind speed (at 10.0 m above the surface) and wave height was 4.23 m/s and 1.12 m, respectively. Maximum wind speeds were 9.70 m/s from the S (Figure 4.1A) which is predominantly onshore. Strong winds from the W were also present for time period one which is offshore. During time period two, the average wind speed and wave height was 3.95 m/s and 1.17 m respectively, with maximum wind speeds of 14.73 m/s from the NNE (Figure 4.1B), which were predominantly offshore. Time period two had stronger and more uniform winds in comparison to time period one. Wave forcing events for the duration of the field study were identified as >2.30 m. At no point during the study did the wave height exceed this threshold, suggesting that the waves were not a dominant forcing agent.

4.2 Dune Volumes

Figure 4.2 shows volumetric percent change for the fenced and control site for time periods one and two. Each site is subdivided into three sections (a, b, and c; Figure 4.2A) to demark changes occurring along the back dune, dune base, and the dune slope for each transect (3D illustration shown in Figure 3.7A). The average change by section is shown in Table 4.1 to assess the holistic geomorphic response that occurred at each site.

During time period one, the sitewide volumetric change within the fenced site was a loss of 18.4% (-26.4 m^3). However, variability occurred within the site. Between fences 9 and 10 along the back dune (section a; Figure 4.2A), the greatest deposition was measured (+60.0%). The greatest erosion (-30.4%) was measured along the dune slope between fences 1 and 2. Sitewide, the average from the dune bases (section b) had the largest percent change at -29.9% (Table 4.1). Erosion was documented on the southwest extent of the site between fences 1 and 4 in proximity to the beach access point (Figure 4.3). Deposition occurred along the shore parallel fence that delineated the landward extent of the site (back dune) and along the dune slope (section c) between fences 4 and 7 (Figure 4.2A).

The control site had a sitewide volumetric loss of 11.2% (-31.2 m^3) during time period one. The site experienced deposition along the landward extent (back dune), which was delineated by vegetation (Figure 4.2B). The back dune experienced the greatest deposition (+50.0%) that occurred between transects 2 and 3. The greatest negative percent change was -23.4%, which occurred along

the dune base between transects 1 and 2. On a sitewide scale, the back dune had the largest percent change at +34.9% (Table 4.1) and the site experienced erosion along the dune base and slope. Data demonstrated that the fenced site experienced a greater percent loss (erosion) in the dune base and dune slope and a lower percent gain (deposition) in the back dune (Table 4.1). The net loss was greater in comparison to the control site when standardizing the percent change.

During time period two, the sitewide volumetric gain within the fenced site was 6.5% (+14.0 m^3). Measurements indicate that deposition occurred within the dune base throughout most of the site and within the dune slope between fences 3 and 6, and 7 and 10 (Figure 4.2C). The greatest positive percent change (deposition) was +48.0% along the dune slope between fences 5 and 6 (Figure 4.2C). The greatest negative percent change (erosion) was -18.0% along the dune slope between fences 1 and 2. The dune base had the greatest percent change at +17.9% (Table 4.1).

The control site had a site-wide volumetric loss of 8.1% (-12.4 m^3). The greatest deposition was +56.0% and was measured in the back dune along the landward extent of the site between transects 3 and 4 at the vegetation line (Figure 4.2D). The greatest erosion (-12.5%) was measured along the dune slope between transects 1 and 2. On a sitewide scale, the back dune had the greatest percent change (-28.6%; Table 4.1). After time period two, data indicated that the fenced site experienced a lower percent loss (erosion) in the back dune and a greater percent gain (deposition) in the dune base and dune

slope (Table 4.1). The fenced site had a net gain, while the control had a net loss. The geomorphic response per section was not consistent throughout the duration of the study and patterns of erosion and deposition varied by time period.

4.3 Erosion Pins

Figure 4.3 shows the percent change measured from the erosion pins for the fenced and control site for time periods one and two. After the first time period, the fenced site experienced deposition in the back dune (section a) along the shore-parallel fence aligned with oblique fences 2-5, and 8-10 (Figure 4.3A). The average percent change within the back dune was +180.0%. Erosion is prevalent along the dune base (section b) for most of the site with an average loss of -375.0% and along the dune slope from fences 1-5 (section c) with an average loss of -25.0% (Figure 4.3A). Changes within the control site after time period one indicate that the back dune (section a) was dominated by deposition (averaging +166.7%; Figure 4.3B). Sections b and c were dominated by erosion with an average loss of -1.7% and -164.0%, respectively (Figure 4.3B).

After time period two, the fenced site experienced an average loss of 2.1% in the back dune, and an average gain of +20.2% and +3.2% at the dune base and dune slope, respectively (Figure 4.3C). Changes within the control site indicate an average gain of +22.9% in the back dune and an average loss of -94.5% in the dune base (Figure 4.3D). An assessment for the dune slope was impeded by a loss of erosion pins by anthropogenic or natural causes; no erosion pins at the dune toe were recovered.

4.4 Sediment Analysis

Table 4.2 summarizes the standard grain distribution statistics, including mean grain size, sorting, and the sieving error for each sample. All samples were well-sorted fine sand. For the duration of the field study, the mean grain size for the fenced site was 0.157 mm. The control site had a slight coarser mean grain size of 0.168 mm. Given the proximity of the sites, and average of D_{50} was assumed for each time period using the data from Table 4.2, with 0.160 mm applied for time period one, and 0.167 mm applied for time period two, respectively. The sorting (σ_g) decreased over time at the control site, but a similar trend was not found at the fenced site.

4.5 Mass Transport Modeling

Table 4.3 shows the results for estimating transport conditions using multiple grain classes when assuming minimum wind speeds necessary for $u_* > u_{*t}$ presented by grain class. The influence of precipitation is also presented. It is assumed that aeolian transport is not possible 24 hours following precipitation.

For time period One, 92 of the 240 hours were estimated as potential time for aeolian sediment transport to occur. There was the highest potential for transport assuming VFS (mean grain size of 0.063 mm), which was 21.7% or 52 of the 240 hours. Fine sand (FS) transport was estimated to take place 39 hours, or 11.1% of the time. Medium sand (MS) is estimated for 0.4% of the total transport time, which equates to 1 hour. Results suggest that based on wind speed measurements, transport cannot occur for coarse sand (CS) or very coarse sand (VCS). Results from sediment samples collected during time period

one (shown in blue; Table 4.3) had an average D_{50} of 0.160 mm. This grain size had an estimated transport of 4.2%, or 10 of the 240 hours.

For time period Two, 172 of the 552 hours considered were estimated as potential time for transport to occur. There was the highest potential for transport assuming VFS (mean grain size of 0.063 mm), which was 16.7% or 92 of the 240 hours. Find sand (FS) transport was estimated to take place 71 hours, or 6.5% of the time. Medium sand (MS) is estimated for 9 hours, or 1.6% of the time. Results suggest that based on wind speed measurements, transport can not occur for coarse sand (CS) or very coarse sand (VCS). Sediment samples collected for time period two (shown in green; Table 4.3) had an average D_{50} value of 0.167 mm. The average D_{50} grain size had an estimated transport of 18 hours, or 3.3% of the time for time period two.

Sediment composition for time period two was dominated by FS (74.2%) and VFS (18.7%). The remaining three sediment grain classes account for less than 10% of the overall composition (Table 4.3). The time (hours) for potential transport was negatively correlated to grain size and resultant threshold shear velocities for time periods one and two.

Table 4.1. Volumetric percent change by section for the fenced and control sites for the duration of the study. Negative values indicate erosion and positive values indicate deposition.

Section	Site	Time period one (9/11/18-9/21/18) (%)	Time period two (9/21/18-10/13/18) (%)
Back dune a	Fenced	+21.1	-17.7
	Control	+34.9	-28.6
Dune base b	Fenced	-29.9	+17.9
	Control	-18.4	-3.5
Dune slope c	Fenced	-20.6	+16.7
	Control	-7.4	-15.2

Table 4.2. Sediment characteristics for the control and fenced site for the three field collection dates. D_{50} is mean grain size (mm), and σ_g is sediment sorting (mm).

Date	Site	D_{50} (mm)	σ_g (mm)	Sieving Error (%)
9/11/218	Fenced	0.150	0.144	1.1
	Control	0.167	0.164	1.6
9/21/18	Fenced	0.157	0.070	0.9
	Control	0.164	0.099	1.3
10/13/18	Fenced	0.165	0.144	0.7
	Control	0.174	0.069	0.5

Table 4.3. Estimated hours of transport ($u_* > u_{*t}$) based on mean grain size in mm. Minimum wind speeds necessary for transport conditions are presented to estimate hours for potential transport. Time excludes measurements within 24 hours of recorded precipitation. VFS is very fine sand, FS is fine sand, MS is medium sand, CS is coarse sand, and VCS is very coarse sand. Values in blue are measured mean grain size for time period one and values in green are measured mean grain size for time period two. The hours of estimated transport for time periods one and two and included in the fine sand (FS) hour counts by time period. Average sediment composition (%) by grain class is presented for both time periods.

Sediment Characteristics			Wind Characteristics		Influence of Precipitation on Mass Transport			
					Time Period One Transport Time		Time Period Two Transport Time	
Grain Size (mm)	AVG Sediment Composition Time Period One (%)	AVG Sediment Composition Time Period Two (%)	Threshold shear velocity (u_{*t}) (m/s)	Minimum wind speed for $u_* > u_{*t}$ (m/s)	Percent	Hours	Percent	Hours
0.063 (VFS)	19.9	18.7	0.117	4.5	21.7	52	16.7	92
0.125 (FS)	72.7	74.2	0.166	6.1	8.3	39	6.2	71
0.160			0.188	6.8	4.2	10	3.4	
0.167			0.192	6.9	3.8		3.3	18
0.250 (MS)	5.2	5.6	0.235	8.2	0.4	1	1.6	9
0.500 (CS)	1.8	0.5	0.332	11.0	0.0	0	0.0	0
1.000 (VCS)	1.3	0.8	0.469	14.6	0.0	0	0.0	0
Time Period One Volume Change (m^3)				Fenced	-26.4 (18.4%)			
				Control	-31.2 (11.2%)			
Time Period Two Volume Change (m^3)							Fenced	+14.0 (6.5%)
							Control	-12.4 (8.1%)

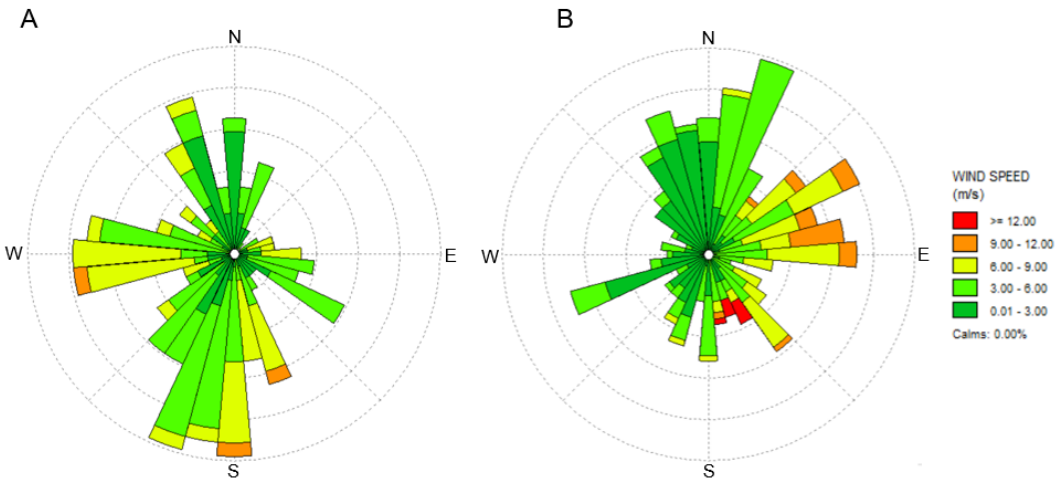

Figure 4.1. Wind roses for time period one (A) and time period two (B) at NOAA's Charleston River Cooper Entrance Station 8665530. Wind speeds are corrected to 10.0 m above the surface using Burt's (2012) wind scaling multiplier.

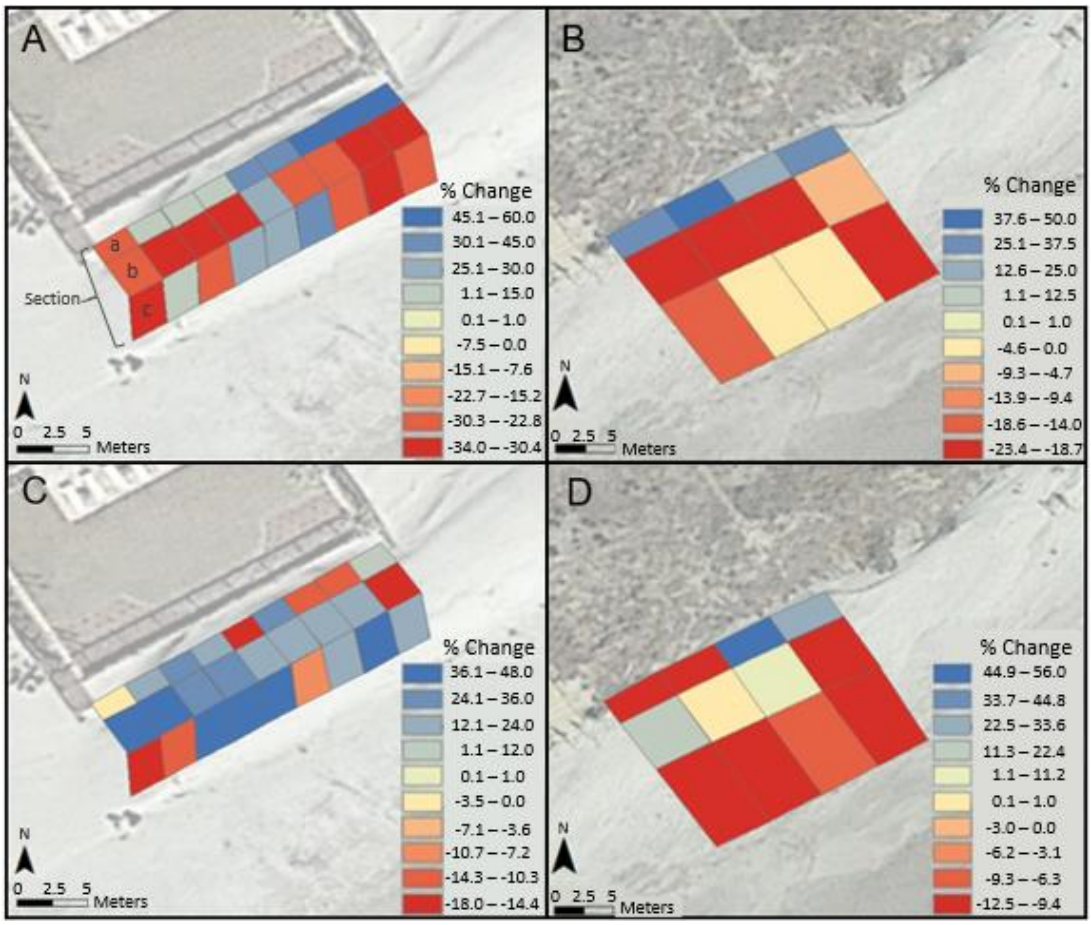

Figure 4.2. Schematics showing volumetric change (%) where positive and negative values indicate deposition and erosion. Sections a-c found in panel A apply to panels B-D. A) Fenced site change during time period one. B) Control site change during time period one. C) Fenced site change during time period two. D) Control site change during time period two.

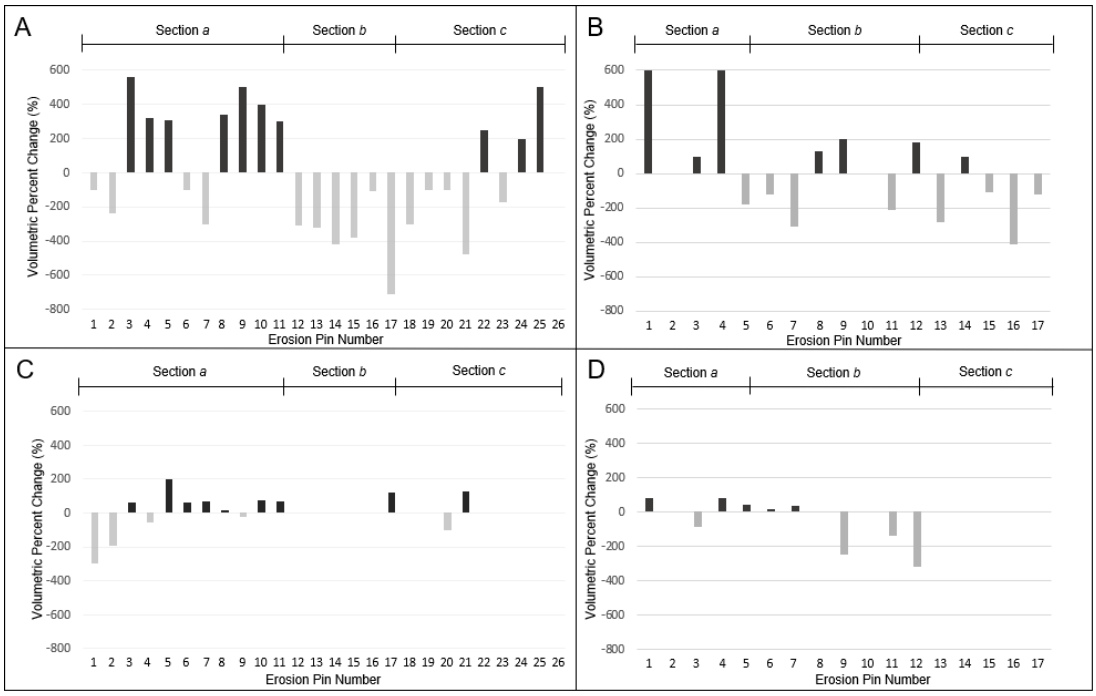

Figure 4.3. Erosion pin percent change for both the fenced and control sites. Missing values indicate that no measurement was taken for that erosion pin. The pins are sorted by section (see section 3.4). A) Percent change after time period one for the fenced site. B) Percent change after time period one for the control site. C) Percent change after time period two for the fenced site. D) Percent change after time period two for the control site.

CHAPTER 5

DISCUSSION

A holistic approach was adopted to assess the post-storm morphological changes that occurred at the fenced and control site during the two time periods considered for this study. Applying equations 2 and 3, the estimated mean and maximum shear velocities for time period one (9/11/2018-9/21/2018) were 0.11 m/s and 0.27 m/s and for time period two (9/21/2018-10/13/2018) were 0.12 m/s and 0.40 m/s. Threshold shear velocity was estimated with equation 2 and was approximately 0.19 m/s for both time periods. Under ideal environmental conditions (Ellis and Sherman, 2013) these values support sediment aeolian transport occurring for the fenced and control site during both time periods. The estimated hours of transport under these ideal conditions is presented (Table 4.3), only dry conditions with uniform grain sizes are considered. Although not measured in this study, conditions such as topographic variability, surface crusting, and wind direction should be considered when further discussing inhibitors to transport. The influence of these additional environmental conditions may explain why time period two had more hours of potential transport, but less volumetric change when compared to time period one (Table 4.3). CoCoRaHs provides a wealth of data but also has its limitations. These data are acquired once per 24 hours at variable times per day. Our choice to exclude transport data for the 24 hours following the ‘day’ CoCoRaHs recorded precipitation is

temporally restrictive. The division of transport hours by grain size identifies the importance of sediment composition for coastal management. For this study, the greatest amount of transport hours occurred for VFS that comprised approximately 20% of the average sediment sample composition. FS, comprising approximately 73% of the sample composition, had 24% fewer estimated transport hours. Managers should be cognizant when considering borrow sites for nourishment projects, or practices such as beach scraping which may alter sediment grain sizes (Bruun, 1983; Ellis and Román-Rivera, 2019), influencing the natural transport rate.

A comparison of storm energetics evaluated the impacts from Hurricanes Florence and Michael on the field sites. An evaluation of wave forcing events (heights >2σ) suggested that waves were not a relevant forcing agent for morphologic change. This was supported by observations in the field, where the wrack line always fell shoreward of the dune toe, even under king tide conditions (Figure 3.2A). We therefore focused our analysis of forcing agents on wind. For time period one, winds (adjusted to 10.0 m above the bed) were onshore and offshore with mean and maximum speeds of 4.23 m/s and 9.7 m/s, respectively. During time period two mean and maximum speeds of 3.95 m/s and 14.73 m/s, respectively, were measured.

The fenced and control sites had net volumetric losses of 26.3 m^3 (8.6%) and 43.6 m^3 (15.6%) at the conclusion of this study. The fenced site displayed differential patterns of erosion and deposition (σ = 14.5% for volumetric change between transects) when compared to the control site (σ = 3.8%) (Figure 4.2).

Data suggested that the greatest morphologic change occurred during time period one. This result was supported by field measurements (Figure 4.2 A; B, Figure 4.3 A; B). However, the inclusion of field photographs (Figure 5.1 A; B; C) indicated that fine-scale depositional patterns were not thoroughly detected by the field measurements and as such, the results should be carefully considered when assessing volumetric change during period two when depositional patterns were most observed. At the conclusion of time period two (Figure 5.1C) results indicated that under maximum wind conditions, greater incipient dune growth was observed in the fenced site while erosion occurred concurrently in the control site (Figure 4.2 C; D). The exception to this occurred along the back dune (section a) where native plants aided in trapping sediment to stabilize and increase dune volume. This role was mimicked at the fenced site by the presence of the shore parallel fence. Field photos and in situ data within section *a* supported this depositional trend and landward migration witnessed at both field sites. The fenced dune site was largely unvegetated, with a stabilizing species appearing between fences 4-5 during time period one, which promoted an increase in volume. This observance supported the previous suggestion that sand fences and vegetation promote dune growth and recovery (Mendelssohn et al., 1991). Deposition was predominantly located around the native vegetation, between the oblique fences, and along the shore parallel fence. These depositional patterns support the functionality of sand fences for dune building and recovery (Miller, Thetford, and Yager, 2001; Khalil, 2008) in environments susceptible to aeolian transport. The depositional patterns and orientation follow

the dominant wind direction observed during Hurricane Michael's path during time period two, supporting that the storm largely influenced the geomorphic change observed at the site.

One of the principle limitations of this study was the length of temporal durations (time periods). This study identified two temporal windows for analysis but there did not allow us to isolate storm-derived morphologic change. Anthropogenic impacts were another limitation. Specifically, the influence of 'human erosion machines' (HEM's; Ellis and Román-Rivera, 2019) as it was particularly evident that the erosion pins were manually removed from section *c* (Figure 3.6B) after time period one. Although these limitations may reduce the accuracy of the measurements presented, they did not hinder the results presented regarding the erosion-accretion dynamics present at each site based on the emplacement of the sand fences and provide further researchers suggestions for improvements.

Figure 5.1. Photos of the fenced site on the three collection dates, featuring the shore parallel and oblique fences. A) Pre-Florence; B) Post-Florence/Pre-Michael; C) Post-Michael

CHAPTER 6

CONCLUSION

This study highlighted the geomorphic impacts of sand fences on a mechanical dune system under the influence of tropical cyclones. Specifically, this study sought to compare the geomorphic changes occurring within a fenced and control site during Hurricanes Florence and Michael along Isle of Palms, South Carolina. To the best of our knowledge, no study has evaluated the post-storm impact of sand fences emplaced pre-storm. Similarly, scant research has evaluated this management technique within a mechanical dune environment that may respond differently than a natural dune environment.

The methodology introduced in this study served to provide a universal, cost-effective process that was appropriate for quick deployment. A combination of field measurements and photographs allowed for a holistic assessment following both time periods that can readily be adopted by citizens or coastal managers.

This study considered two temporal durations: time period one (9/11/2018-9/21/2018) that included Hurricane Florence and time period two (9/21/2018-10/13/2018) that included Hurricane Michael. No forcing (>2σ) wave events were recorded.

Results showed that during time period one, erosion was prevalent at both field sites and that after time period two, deposition was present at the fenced site. Overall, the fenced site had a lower net loss at the conclusion of the study. The dune formations resulting from time period two suggest that sand fences can be effective if emplaced pre-storm, rather than reserved for post-storm recovery. It also supports their resilience to high wind conditions.

The question of sand fence efficacy is important to managers and homeowners seeking to adopt this cost-effective technique. This study introduces sand fence persistence and response to storm conditions, providing one step in the effort to understand fence efficacy. Future steps to identify fence lifespan and dune growth would be beneficial in providing regulatory guidelines for fence deployment. This would allow a further understanding of the role this management technique may have in a natural or mechanical dune environment.

LITERATURE CITED

Bagnold, R. (1936). The movement of desert sand. Proceedings of the Royal Society of London. Series A, Mathematical and Physical Sciences, 157, pp. 594-620.

Bagnold, R. (1937). The Size Grading of Sand by Wind. Proc. Roy. Soc. A, 157. *Geog. J*, 89, 428.

Bagnold, R. (1941). The physics of blown sand and desert dunes. Chapman and Hall, London. 265 pp.

Bruun, P. (1983). Beach Scraping – Is it Damaging to Beach Stability? *Coastal Engineering, 7,* 167-173.

Burt, S. *The Weather Observer's Handbook.* New York: Cambridge University Press. 2012.

Claudino-Sales, V., Wang, P., & Horwitz, M. (2008). Factors Controlling the Survival of Coastal Dunes during Multiple Hurricane Impacts in 2004 and 2005: Santa Rosa Barrier Island, Florida. *Geomorphology, 95*(3-4), 295-315. https://doi:10.1016/j.geomorph.2007.06.004.

Coastal Science and Engineering (CSE). (2017). Hurricane Irma Damage Assessment. 6 pp.

Conathan, M., Buchanan, J., & Polefka, S. (2014). The Economic Case for Restoring Coastal Ecosystems. Center for American Progress and Oxfam America, 54 pp.

Conaway, C., & Wells, J. (2005). Aeolian Dynamics along Scraped Shorelines, Bogue Banks, North Carolina. *Journal of Coastal Research, 212*, 242-54. https://doi:10.2112/01-089.1.

Ellis, J., & Román-Rivera, M. (2019). Assessing Natural and Mechanical Dune Performance in a Post-Hurricane Environment. *Journal of Marine Science and Engineering, 7*(126), 1-15.

Ellis, J., & Sherman, D. (2013). Fundamentals of Aeolian Transport: Wind-Blown Sand. In: John F. Shroder (ed.) Treatise on Geomorphology, Volume 11, pp. 85-108. Sand Diego: Academic Press. https://doi:10.1016/B978-0-12-374739-6.00299-2.

Fico, C. (1980). Influence of Wave Refraction on Coastal Geomorphology - Bull Island to Isle of Palms, South Carolina. Columbia, SC: University of South Carolina.

Grafals-Soto, R. (2012). Effects of sand fences on coastal dune vegetation distribution. Geomorphology, 145-146, 45-55.

Grafals-Soto, R., & Nordstrom, K. (2009). Sand Fences in the Coastal Zone: Intended and Unintended Effects. *Environmental Management, 44*(3), 420-29. https://doi:10.1007/s00267-009-9331-7.

Hal, M., & Halsey, S. (1991). Comparison of overwash penetration from Hurricane Hugo and pre-storm erosion rates for Myrtle Beach and North Myrtle, South Carolina. *Journal of Coastal Research, 8*, 229–236 (Special Issue).

Hayes, M. (2010). Shore of South Carolina: geomorphology and costal processes. *Shore and Beach*, 78(3), 3-19.

Herrmann, H., & Sauermann, G. (2000). The shape of dunes. *Physica A, 283*, 24-30.

Hotta, S., & Horikawa, K. (1991). Function of Sand Fence Placed in Front of Embankment. *Coastal Engineering 1990*. https://doi:10.1061/9780872627765.211.

Houser, C., Hapke, C., & Hamilton, S. (2007). Controls on Coastal Dune Morphology, Shoreline Erosion and Barrier Island Response to Extreme Storms. *Geomorphology, 100*(3-4), 223-40. https://doi:10.1016/j.geomorph.2007.12.007.

Houser, C., Wernette, P., Rentschlar, E., Jones, H., Hammond, B., & Trimble, S. (2015). Post-storm beach and dune recovery: Implications for barrier island resilience. *Geomorphology, 234*, 54-63.

Huang, W., & Yim, J. (2014). Sand Dune Restoration Experiments at Bei-Men Coast, Taiwan. *Ecological Engineering, 73*, 409-20. https://doi:10.1016/j.ecoleng.2014.09.038

IOP, (2018). Hurricane Michael. City of Isle of Palms. Accessed October 18, 2018. https://www.iop.net/hurricane-michael-

Jackson, N., and Nordstrom, K. (2011). Aeolian sediment transport and landforms in managed coastal systems: A review. *Aeolian Research, 3*(2), 181-196. https://doi.org/10.1016/j.aeolia.2011.03.011

Kadib, A. (1965). A function for sand movement by wind (No. HEL-2-12). California Univ Berkeley Hydraulic Engineering Lab.

Kana, T. (1988). Beach Erosion in South Carolina. Charleston, SC: South Carolina Sea Grant Consortium.

Kana, T., & Svetlichny, M. (1982). Artificial Manipulation of Beach Profiles. Paper presented at the 18th International Conference on Coastal Engineering, Cape Town, South Africa. November 14-19.

Katuna, M. (1991). The Effects of Hurricane Hugo on Isle of Palms, South Carolina: From Destruction to Recovery. Journal of Coastal Research, 8, 263-273.

Kawamura, R. (1951). Study on sand movement by wind. Reports of Physical Sciences Research Institute of Tokyo University, 5(3-4), 95-112 (translated from Japanese by National Aeronautic and Space Administration (NASA), Washington, DC, 1972).

Kerhin, R., & Halka, J. (1981). The effectiveness of beach scraping as a method of erosion control: Topsail Beach, North Carolina. Unpublished M.S. Thesis, University of North Carolina, 72 pp.

Khalil, S. (2008). The Use of Sand Fences in Barrier Island Restoration: Experience on the Louisiana Coast. *System-Wide Water Resources Program*, 1-23.

Lentz, E., Hapke, C., Stockdon, H., & Hehre, R. (2013). Improving understanding of near-term barrier island evolution through multi-decadal assessment of morphologic change. Marine *Geology, 337*, 125-139.

Lettau, H., & Lettau, K. (1978). Experimental and micrometerological field studies of dune migration. In: Lettau, K., Lettau, H.H. (Eds.), Exploring the World's Driest Climate. University of Wisconsin-Madison, Madison, pp. 110-147.

Li, B., & Sherman, D. (2015). Aerodynamics and Morphodynamics of Sand Fences: A Review. *Aeolian Research 17*, 33-48. https://doi:10.1016/j.aeolia.2014.11.005.

Lima, I., Ascânio, D., Araújo, E., Parteli, R., Andrade, J., & Herrmann, H. (2017). Optimal Array of Sand Fences. *Scientific Reports,* 7. https://doi:10.1038/srep45148.

Lindemer, C., Plant, N., Puleo, J., Thompson, D., & Wamsley, T. (2010). Numerical Simulation of a Low-lying Barrier Islands Morphological Response to Hurricane Katrina. *Coastal Engineering 57*(11-12), 985-95. https://doi:10.1016/j.coastaleng.2010.06.004.

Lindquist, N., and Manning, L. (2001). Impacts of Beach Nourishment and Beach Scraping on Critical Habitat and Productivity of Surf Fishes. Final report.

Long, J., De Bakker, A., & Plant, N. (2014). Scaling Coastal Dune Elevation Changes across Storm-impact Regimes. *Geophysical Research Letters, 41*(8), 2899-906. https://doi:10.1002/2014gl059616.

López, R., & Marcomini, S. (2006). Monitoring the Foredune Restoration by Fences at Buenos Aires Coast. *Journal of Coastal Research, 39*, 955-958.

Mendelssohn, I., Hester, M., Monteferrante, F., & Talbot, F. (1991). Experimental Dune Building and Vegetative Stabilization in a Sand-Deficient Barrier Island Setting on the Louisiana Coast, USA. *Journal of Coastal Research, 7*(1), 137-49.

Miller, D., Thetford, M., & Yager, L. (2001). Evaluation of Sand Fence and Vegetation for Dune Building following Overwash by Hurricane Opal on Santa Rosa Island, Florida. *Journal of Coastal Research*, *14*(4), 936-48.

NOAA, (2016). Historical Hurricane Tracks: South Carolina. Accessed October 1, 2018.

NOAA, (2018). National Data Buoy Center Continuous Wind Data: Charleston River Cooper Entrance, SC, September-October 2018. Accessed October 5, 2018.

Nordstrom, K., & Jackson, N. (2017) Offshore Aeolian Sediment Transport across a Human-modified Foredune. *Earth Surface Processes and Landforms, 43*(1), 195-201. https://doi:10.1002/esp.4217.

Nordstrom, K., Jackson, N., Freestone, A., Korotky, K., & Puleo, J. (2012). Effects of beach raking and sand fences on dune dimensions and morphology. *Geomorphology, 179*, 106-115.

NWS, 2018. Charleston Daily Precipitation Data. Accessed November 3, 2018.

Ocean and Coastal Resource Management (OCRM). 2018. “How to Build a Dune.” South Carolina Department of Health and Environmental Control. http://www.scdhec.gov/environment/docs/dunes_howto.pdf

Peterson, C., Hickerson, H., Johnson, G. (2000). Short-term consequences of nourishment and bulldozing on the dominant large invertebrates of the sandy beach. *Journal of Coastal Research, 16*, 368-378.

Portz, L., Manzolli, R., Hermanns, L., & Alcántara Carrió, J. (2015). Evaluation of the Efficiency of Dune Reconstruction Techniques in Xangri-lá (Rio Grande Do Sul, Brazil). *Ocean & Coastal Management, 104*, 78-89. https://doi:10.1016/j.ocecoaman.2014.12.005.

Psuty, N. (2008). The Coastal Foredune: A Morphological Basis for Regional Coastal Dune Development. Chapter in Ecological Studies, vol. 171.

Pye, K., & Tsoar, H. *Aeolian sand and sand dunes*. Springer Netherlands. 1990.

Sallenger, A. (2000). Storm Impact Scale for Barrier Islands. *Journal of Coastal Research, 16*(3), 890-95.

Savage, R. (1962). Experimental Study of Dune Building with Sand Fences. *Coastal Engineering,* 380-396.

Smyth, T., and Hesp, P. (2015). Aeolian dynamics of beach scraped ridge and dyke structures. *Coastal Engineering, 99*, 38-45.

Stephen, M., Brown, P., FitzGerald, D., Hubbard, D., & Hayes, M. (1975). Beach Erosion Inventory of Charleston County, South Carolina: A Preliminary Report. Charleston, SC: South Carolina Sea Grant Program.

Thieler, E., and Young, R. (1991). Quantitative Evaluation of Coastal Geomorphological Changes in South Carolina After Hurricane Hugo. *Journal of Coastal Research*, *8*, 187-200.

Van der Laan, J., Heino, A., & Waard, D. (1997) A Simple Procedure for the Assessment of Acceptance of Advanced Transport Telematics. *Transportation Research Part C: Emerging Technologies, 5*(1), 1-10. https://doi:10.1016/s0968-090x(96)00025-3.

Wells, J., and McNinch, J. (1991). Beach Scraping in North Carolina with Special Reference to its Effectiveness During Hurricane Hugo. Journal of Coastal Research, 8, 249-261.

White, B. (1979). Soil transport by wind on Mars. Journal of Geophysical Research, 84, 4643-4651.

Zaghloul, N. (1997). Sand Accumulation around Porous Fences. *Environmental Modelling & Software, 12*(2-3), 113-34. https://doi:10.1016/s1364-8152(96)00052-7.

Zhang, K., Douglas, B., & Leatherman, S. (2002). Do Storms Cause Long-Term Beach Erosion along the U.S. East Barrier Coast? *The Journal of Geology, 110*(4), 493-502.